Electron-scale electrostatic solitary waves and shocks: the role of superthermal electrons

S. Sultana* and I. Kourakis†

Centre for Plasma Physics, Department of Physics and Astronomy,
Queen's University Belfast, BT7 1NN Northern Ireland, UK
(Dated: February 23, 2012)

The propagation of electron-acoustic solitary waves and shock structures is investigated in a plasma characterized by a superthermal electron population. A three-component plasma model configuration is employed, consisting of inertial ("cold") electrons, inertialess κ (kappa) distributed superthermal ("hot") electrons and stationary ions. A multiscale method is employed, leading to a Korteweg-de Vries (KdV) equation for the electrostatic potential (in the absence of dissipation). Taking into account dissipation, a hybrid Korteweg-de Vries–Burgers (KdVB) equation is derived. Exact negative-potential pulse- and kink-shaped solutions (shocks) are obtained. The relative strength among dispersion, nonlinearity and damping coefficients is discussed. Excitations formed in superthermal plasma (finite κ) are narrower and steeper, compared to the Maxwellian case (infinite κ). A series of numerical simulations confirms that energy initially stored in a solitary pulse which propagates in a stable manner for large κ (Maxwellian plasma) may break down to smaller structures or/and to random oscillations, when it encounters a small-κ (nonthermal) region. On the other hand, shock structures used as initial conditions for numerical simulations were shown to be robust, essentially responding to changed in the environment by a simple profile change (in width).

I. INTRODUCTION

Electron-acoustic (EA) waves (EAWs) occur in a plasma containing two distinct temperature electrons (here to be referred to as "hot" and "cold" electrons) [1–6]. This is a high-frequency mode, for which inertia is provided by the cold electron motion, while the restoring force comes from the hot electron thermal pressure. Ions may be safely assumed to be stationary, simply maintaining the charge neutrality of the plasma. The frequency of EAWs lies in the range between the plasma frequency of the cold and hot electron components. As a matter of fact, Landau damping is minimized if the cold electron population consists of 20% to 80% of the total number of electrons [7–9], i.e., for values of the cold-to-hot electron density ratio in the range $0.25 \leq n_{c0}/n_{h0} \leq 4$. The signature of EAWs has been traced in the middle-altitude cusp region [10] by instruments on board CLUSTER spacecraft and also in the laboratory [11]. EAWs have also been observed in particle-in-cell simulations as a result of beam-driven instabilities [12, 13]. Electron acoustic waves can be driven by electron beams in a plasma comprising a hot and a cold electron population [12]. Furthermore, such waves can also be driven by ion beams, where a cold and a hot electron component naturally arises when the electrostatic instability saturates [13]. After the collapse of an initial (large) periodic train of electron phase space holes, smaller and stable electron acoustic solitary structures may survive and propagate in the hot electron distribution. In that context, the hot electron population is provided by electrons trapped by the large waves (we refer an interested reader to the discussion in Ref. [13]).

Various theoretical investigations have focused on the linear [2, 3, 7] and nonlinear [5, 6, 8, 9, 14–18] dynamics of EAWs. In a space-plasma theoretical context, the occurrence of large-amplitude EA nonlinear structures was investigated by Singh and Lakhina [19], who considered the relevance of the theory with broadband electrostatic noise (BEN) emission observed in the auroral zone and in other regions of the Earth's magnetosphere [20–23]. Remarkably, positive-potential solitary excitations may also exist in the presence of an electron beam [19], or in the presence of a vortex-type electron distribution, as predicted by a small amplitude model [6, 14]. The nonlinear properties of EA solitary waves have also been investigated in a nonthermal plasma [14, 16, 17] by taking into account nonthermality through a vortex-like [14] or via a Cairns type [16]. A similar study relying on a pseudopotential analysis and adopting a κ type distribution function for the hot electrons has been presented, independently, in Refs. 17 and 18. The modulational instability of EA wavepackets and the occurrence of bright/dark-type envelope solitons were studied in Refs. [5] and [24] from first principles.

Particle distribution in a plasma near equilibrium is often assumed to be Maxwellian, for modeling purposes. However, numerous space plasma observations [25–27] and laboratory experiments [28–30] indicate the presence of highly energetic ("superthermal") particles. This phenomenon can be efficiently modeled by a generalized Lorentzian or $\kappa-$ distribution [31–33], where the real parameter κ measures the

─────────

*Email: basharminbu@gmail.com
†Email: i.kourakis@qub.ac.uk; IoannisKourakisSci@gmail.com; www.kourakis.eu

strength of excess superthermality (the smaller the value, the larger the deviation from a Maxwellian, in fact attained for infinite κ). Plasmas with superthermal components (electrons and/or ions) have received a great interest recently, both theoretically [8, 9, 24, 34, 35] and experimentally [36]. As expected, the dynamics of plasma waves are significantly affected by superthermality. Large-amplitude ion-acoustic solitons in magnetized superthermal plasmas was considered in Ref. [34], where the properties and the existence regions of solitary structure were shown to change drastically (with respect to the standard Maxwellian description). Modulated EA wavepackets in superthermal plasma were also investigated in Ref. [24], where the stability profile was shown to be dramatically modified by superthermality. The linear properties of EAWs in κ-distributed plasmas were established via a rigorous kinetic approach by Mace *et al* [8] and were later revisited by Baluku *et al* [9], who showed that EAWs can survive Landau damping in a wide range of wavenumbers and κ parameter values.

According to the standard nonlinear description, small-amplitude solitary waves are usually described via a Korteweg - de Vries (KdV) equation, which models the balance between nonlinearity and dispersion necessary for the formation of stable localized structures. In dissipative systems, the same analytical (perturbation) technique gives rise to a KdV-Burgers equation, featuring an extra term in account of dissipation, with the anticipation that nonlinearity may be balanced by the combined effect of dispersion and dissipation to form kink-shaped shock excitations. Dissipative effects in plasmas might be due to the inter-particle collisions, to Landau damping or to kinematic fluid viscosity, e.g., due to shear stress of the inertial fluid motion. This situation has been considered for ion-acoustic [37, 38] waves, and also for dust-acoustic [39–41] or for dust ion-acoustic [40, 42] waves in dusty plasmas. Interestingly, Velikovich [43] showed that the electron-ion collision cross-section is higher than its ion-ion counterpart by a factor Z^2 in high Z plasmas (where the electron density is Z times larger than the ion density). Electron viscosity was found to exceed ion viscosity considerably, e.g., for isothermal plasma ($T_i = T_e$) with $Z > 5$. Furthermore, electron viscosity was shown to dominate for higher electron temperature values and for higher Z [43]. Relying on the investigation in Ref. [43], we are interested in a plasma situation where electron-ion collision cross-section is larger than the ion-ion collision cross-section and the electron viscosity can be taken into account. Accordingly, energy dissipation due to electron-ion collisions will be considered in the following. As regards the electron-acoustic mode, this situation is analogous to ion-acoustic waves (though occurring on a different frequency scale), here letting the cold electrons play the role of the ions and their kinematic viscosity (due to dynamic viscosity) damping their fluid motion in the long wavelength limit. For simplicity, the kinematic viscosity is considered constant throughout this work.

In this work, we take into account the dissipation effect on small-amplitude electron-acoustic shock (where solitary structures are recovered in the absence of dissipation), in a plasma characterized by a superthermal electron distribution. Throughout this work, we shall restrict ourselves implicitly in the existence region for EAWs proposed in earlier works [7, 8], where Landau damping is minimized. This manuscript is arranged in the following manner. Our fluid model is presented in Section II and analyzed the linear limit in Sec. III. The derivation of a KdVB equation via a reductive perturbation approach is undertaken in Sec. IV. Sec. V is dedicated for brief discussions about KdV equation and its solution. The analytical solution of KdVB equation and the behavior of the associated electric field is presented and discussed briefly in Sec. VI. A parametric investigation is carried out in Sec. VII, based on different relevant parameters for the model and a brief numerical results for EA solitary waves and shocks are presented in section VIII. Finally, our results are summarized in the concluding section IX.

II. THE MODEL

We consider a three-component plasma, which is composed of inertial (cold) electrons, kappa-distributed (hot) electrons, and positive ions. It is understood that the phase speed of electron-acoustic excitations is larger than the thermal speed of both cold electrons and ions, and is much smaller than the thermal speed of hot electrons, i.e., $v_{th,c}, v_{th,i} \ll v_{ph} \ll v_{th,h}$ (where the indices c, h and i represent the cold electrons, hot electrons and ions, respectively). Accordingly, the hot electron inertia can be neglected, while the ions can be safely assumed to be immobile (simply maintaining the charge neutrality of the system).

The fluid evolution equations for the (cold) electron fluid read:

$$\frac{\partial n_c}{\partial t} + \frac{\partial (n_c u_c)}{\partial x} = 0, \qquad (1)$$

$$\frac{\partial u_c}{\partial t} + u_c \frac{\partial u_c}{\partial x} = \frac{e}{m_e} \frac{\partial \Phi}{\partial x} + \eta_c \frac{\partial^2 u_c}{\partial x^2}, \qquad (2)$$

where n_c, u_c and Φ represent the cold electron density, velocity, and the electrostatic potential, respectively (m_e is the electron mass). The cold-electron pressure effect has been neglected. The system is closed by Poisson's equation

$$\frac{\partial^2 \Phi}{\partial x^2} = 4\pi e \left[n_c + n_{h0} f(\Phi) - Z_i n_{i0} \right], \qquad (3)$$

where the "hot" electron distribution function $f(\Phi)$ is

given by

$$f(\Phi) = \left[1 - \frac{e\Phi}{k_B T_h(\kappa - 3/2)}\right]^{-\kappa+1/2}, \qquad (4)$$

as obtained by integrating the known form of the κ (kappa) distribution function [33]. The parameter κ here measures the strength of superthermality. Smaller values of κ represent a stronger superthermality; the Maxwellian distribution is recovered in the limit $\kappa \to \infty$ [27, 32] (and in fact practically for κ above, say, 10). Obviously, $\kappa > 3/2$ for a physically acceptable distribution. Here T_h is the characteristics hot electron "temperature" (a real constant) and the subscript "0" refers to equilibrium (k_B is the Boltzmann constant). We have defined the electron kinematic viscosity $\eta_c = \mu_c/m_e n_{c0}$, in terms of the dynamic viscosity μ_c.

A scaled (dimensionless) set of equations is obtained by normalizing all variables by appropriate quantities,

$$\frac{\partial n}{\partial t} + \frac{\partial (nu)}{\partial x} = 0, \qquad (5)$$

$$\frac{\partial u}{\partial t} + u\frac{\partial u}{\partial x} = \frac{\partial \phi}{\partial x} + \eta\frac{\partial^2 u}{\partial x^2}, \qquad (6)$$

$$\frac{\partial^2 \phi}{\partial x^2} \approx \beta(n-1) + c_1\phi + c_2\phi^2. \qquad (7)$$

Here the cold electron number density n, velocity u and electrostatic potential ϕ are normalized by the equilibrium number density n_{c0}, the hot electron thermal speed $v_0 = (k_B T_h/m_e)^{1/2}$ and $\Phi_0 = k_B T_h/e$, respectively. The space x and the time t variables are scaled by the hot electron screening length $\lambda_{D,h} = (k_B T_h/4\pi n_{h0}e^2)^{1/2}$ and by the hot electron plasma period (inverse frequency) $\omega_{p,h}^{-1} = (4\pi n_{h0}e^2/m_e)^{-1/2}$, respectively. The normalized kinematic viscosity reads $\eta = \eta_c/\omega_{ph}\lambda_{D,h}^2$. We have also defined the parameter $\beta = n_{c0}/n_{h0}$, which denotes the cold-to-hot electron density ratio. Note that the superthermal distribution information is now "hidden" in the coefficients

$$c_1 = \frac{\kappa - 1/2}{\kappa - 3/2}, \qquad c_2 = \frac{c_1(\kappa + 1/2)}{2(\kappa - 3/2)}. \qquad (8)$$

As expected, the Maxwellian limit is recovered for $\kappa \to \infty$ ($c_1 \to 1$, $c_2 \to 1/2$, viz., $e^\phi \simeq 1 + \phi + \phi^2/2$).

III. LINEAR ANALYSIS

Linearizing the system of evolution equations, we obtain a dispersion relation in the form:

$$\omega^2 = \frac{\beta k^2 \omega_{p,h}^2}{k^2 + (\sqrt{c_1}/\lambda_{D,h})^2}, \qquad (9)$$

where we have restored dimensions for a while, for physical transparency. This relation is analyzed thoroughly in Ref. [24], so only the basic information is presented here. Eq. (9) can be written in

the form $\omega^2 = \omega_{p,c}^2/[1 + 1/k^2(\lambda_D^{(\kappa)})^2]$, where $\omega_{p,c} = (4\pi n_{c0}e^2/m_e)^{1/2}$ is the cold electron plasma frequency and $\lambda_D^{(\kappa)} = \left[(\kappa-3/2)/(\kappa-1/2)\right]^{\frac{1}{2}} \lambda_{D,h}$ is the effective screening length due to excess superthermality. The dispersion relation (9) is in agreement with Eq. (3) in Ref. [8]. Importantly, the charge screening length is reduced due to superthermality (viz. $\lambda_D^{(\kappa)} < \lambda_D^{(\infty)}$), as pointed out in Refs. [8] and [24].

In the long wavelength limit (i.e., for $k \ll (\lambda_D^{(\kappa)})^{-1}$), Eq. (9) reads

$$\frac{\omega}{k} \simeq \sqrt{\frac{\beta}{c_1}}\,\omega_{p,h}\,\lambda_{D,h} \simeq v_{ph}^{(\kappa)}, \qquad (10)$$

where the $\kappa-$ dependent phase speed is defined as $v_{ph}^{(\kappa)} = \sqrt{\beta/c_1}\,v_0$ (cf. our definition above), in exact agreement with the EA speed defined in Ref. [8]. The EA phase speed is substantially affected by the superthermality parameter κ and by the cold-to-hot electron density ratio β (as shown in Fig. 1). It may be added, for rigor, that we have implicitly considered a phase speed much lower than the hot electron thermal speed, in order to validate the fluid description [1] for the cold electrons. The requirement ensuring the validity of our model thus translates as:

$$\frac{\beta}{c_1} \ll 1, \qquad \Rightarrow \beta \ll \frac{\kappa - 1/2}{\kappa - 3/2}. \qquad (11)$$

We have therefore considered values of the cold-to-hot electron density ratio β obeying Eq. (11), for the respective values of the superthermality parameter κ, both in our linear and nonlinear analyses. In particular, for the values considered e.g. in Figure 1 ($\kappa = 3$, 5 and 100), (11) implies $\beta \ll 1.67$, 1.29 and 1, respectively. The fluid approximation is therefore valid for small β values, while for larger ones one may have to resort to a kinetic approach. We note here that the RHS of (11) equals 1 in Maxwellian plasma, but in kappa-superthermal plasma the RHS can be quite higher, depending on the superthermality index.

IV. MULTISCALE ANALYSIS: DERIVATION OF A KORTEWEG-DE VRIES – BURGERS EQUATION IN THE GENERAL (DISSIPATIVE) CASE

In search of small-amplitude stationary-profile electrostatic waves, we shall adopt the stretched coordinates [44, 45]:

$$\xi = \epsilon^{1/2}(x - v_s t), \qquad \tau = \epsilon^{3/2}t, \qquad (12)$$

————

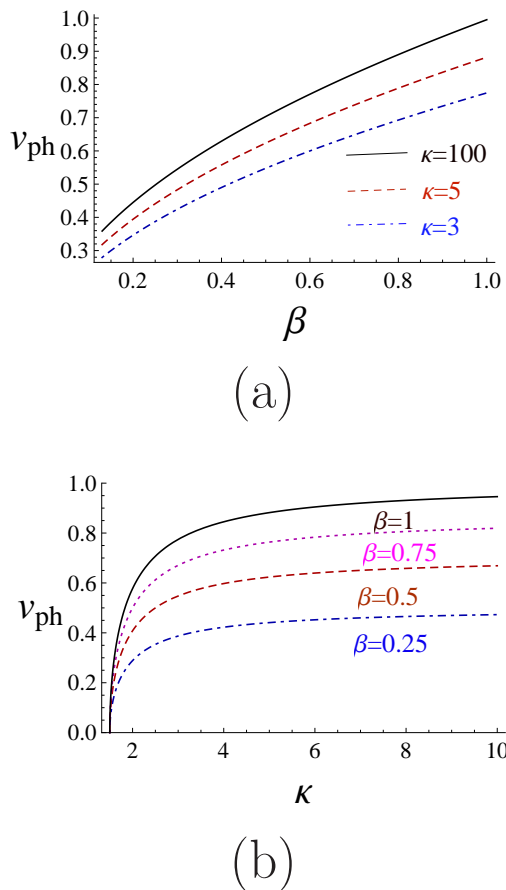[1] Eq. (9) can be obtained from Eq. (3) in Ref. [8] upon neglecting the second term in the numerator therein.

4

FIG. 1: (Color online) The EAW phase velocity is depicted versus (a) the cold-to-hot electron density ratio β, for different κ values; (b) the superthermality parameter κ, for different β.

where ϵ ($\ll 1$) is a small (real) parameter and v_s is the EA shock speed (to be interpreted as the phase velocity). We recall that this stretching is valid for nonlinear waves propagating near the sound speed [44]. In order to match the dissipative terms arising within our expansion, we also assume a weak damping due to the cold electron kinematic viscosity by considering $\eta = \epsilon^{1/2}\eta_0$. This scaling assumption, at this stage motivated by analytical convenience (in view of matching the various mechanisms involved in the dynamics), will be justified by the outcome of the analysis (to be discussed below). This hypothesis also reflects the fact that dissipation is assumed to be (small but) finite, entering the nonlinear dynamics, though too weak to be manifested in the linear regime.

From Eq. (12) we can write

$$\frac{\partial}{\partial t} = \epsilon^{3/2}\frac{\partial}{\partial \tau} - \epsilon^{1/2}v_s\frac{\partial}{\partial \xi}, \qquad \frac{\partial}{\partial x} = \epsilon^{1/2}\frac{\partial}{\partial \xi} . \quad (13)$$

Now we expand the dependent variables n, u and ϕ

near their equilibrium values in a power series in ϵ as

$$n = 1 + \epsilon n_1 + \epsilon^2 n_2 + \epsilon^3 n_3 + \cdots , \qquad (14)$$
$$u = \epsilon u_1 + \epsilon^2 u_2 + \epsilon^3 u_3 + \cdots , \qquad (15)$$
$$\phi = \epsilon \phi_1 + \epsilon^2 \phi_2 + \epsilon^3 \phi_3 + \cdots . \qquad (16)$$

Combining the expressions (13) - (16) into Eqs. (5) - (7) provides the first order perturbations n_1, u_1 and the EAW phase velocity v_{ph}:

$$n_1 = -\phi_1/v_s^2 , \qquad u_1 = -\phi_1/v_s , \qquad v_s = \sqrt{\beta/c_1} . \qquad (17)$$

Interestingly, the latter expression allows us to identify v_s as the phase speed $v_{ph}^{(\kappa)}$ obtained in (10) above. This fact is an intrinsic element in the method, and was expected.

Balancing the coefficients in order $\epsilon^{5/2}$ from Eqs. (5) and (6), and in $\sim \epsilon^2$ from Eq. (7), we obtain

$$-\frac{1}{v_s^2}\frac{\partial \phi_1}{\partial \tau} - v_s\frac{\partial n_2}{\partial \xi} + \frac{2}{v_s^3}\phi_1\frac{\partial \phi_1}{\partial \xi} + \frac{\partial u_2}{\partial \xi} = 0 , \quad (18)$$

$$-\frac{1}{v_s}\frac{\partial \phi_1}{\partial \tau} - v_s\frac{\partial u_2}{\partial \xi} + \frac{1}{v_s^2}\phi_1\frac{\partial \phi_1}{\partial \xi} - \frac{\partial \phi_2}{\partial \xi}$$
$$+\frac{\eta_0}{v_s}\frac{\partial^2 \phi_1}{\partial \xi^2} = 0 , \qquad (19)$$

$$\frac{\partial^2 \phi_1}{\partial \xi^2} - \beta n_2 - c_1\phi_2 - c_2\phi_1^2 = 0 . \qquad (20)$$

Combining Eqs. (18)-(20), we obtain an evolution equation for the lowest-order electrostatic potential disturbance ϕ_1 in the form:

$$\frac{\partial \phi_1}{\partial \tau} + A\phi_1\frac{\partial \phi_1}{\partial \xi} + B\frac{\partial^3 \phi_1}{\partial \xi^3} = C\frac{\partial^2 \phi_1}{\partial \xi^2} . \qquad (21)$$

This equation bears the general form of a Korteweg – de Vries Burgers (KdVB) equation. Identifying various terms, we distinguish:
— a nonlinearity term

$$A = -\frac{3}{2}\sqrt{\frac{c_1}{\beta}} - \frac{c_2}{c_1^{3/2}}\sqrt{\beta}$$
$$= -\frac{3}{2}\sqrt{\frac{1-2\kappa}{\beta(3-2\kappa)}} - \frac{\sqrt{\beta}(1+2\kappa)}{4\kappa-2}\sqrt{1 + \frac{2}{2\kappa-3}} (22)$$

resulting in wave steepening;
— a dispersion term

$$B = \frac{1}{2}\frac{\sqrt{\beta}}{c_1^{3/2}} = \frac{\sqrt{\beta}}{2(1+\frac{2}{2\kappa-3})^{3/2}} , \qquad (23)$$

responsible for wave broadening in Fourier space, and
— a dissipative (damping) term

$$C = \frac{\eta_0}{2} , \qquad (24)$$

leading to wave attenuation (decay) in space. Interestingly, the latter two coefficients B and C are always positive (as intuitively expected), while A is negative. It will be shown below that the sign of A defines

the polarity of soliton and shock excitations sustained in the plasma, thus (A being negative) only negative pulses and kink-shaped potential jumps are prescribed within the plasma model considered here.

Importantly, both coefficients A and B depend on the superthermality parameter κ (via c_1, c_2; see the definitions in (8) above). The two coefficients are depicted in Figs. 2 and 3. The variation trend in κ differs between the two competing mechanisms: the nonlinear coefficient A increases in absolute value, whereas the dispersive coefficient B decreases, as κ acquires lower values (*aka*, deviation from Maxwellian behavior). Therefore, superthermality (low κ) results in a loss of balance between dispersion and nonlinearity: assuming a soliton-shaped initial condition, a change in κ would result in loss of ability to sustain its shape, and energy breakdown to smaller structures or/and to random oscillations.
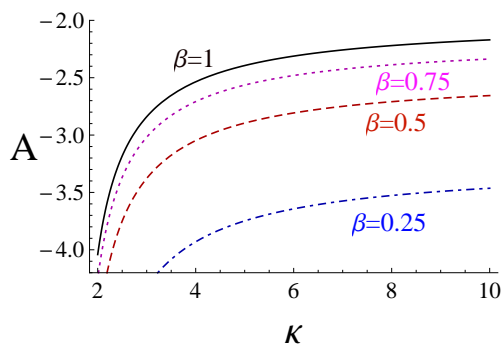
(a)
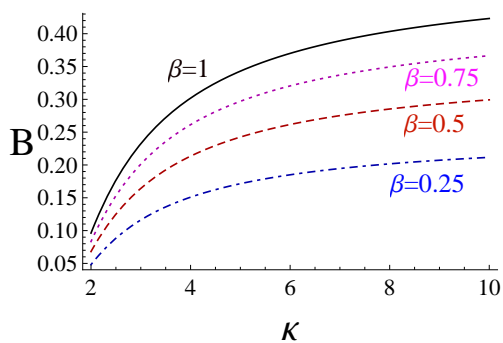
(b)

FIG. 2: (Color online) The nonlinearity coefficient A and the dispersion coefficient B are shown versus κ for different values of β. The curves correspond, top to bottom, to: $\beta = 1$ (solid black curve); $\beta = 0.75$ (dotted magenta curve); $\beta = 0.5$ (dashed red curve) and $\beta = 0.25$ (dot-dashed blue curve).
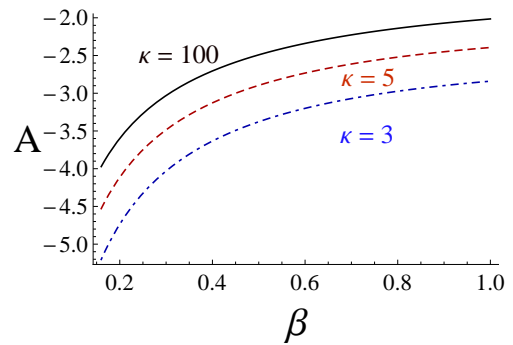
(a)
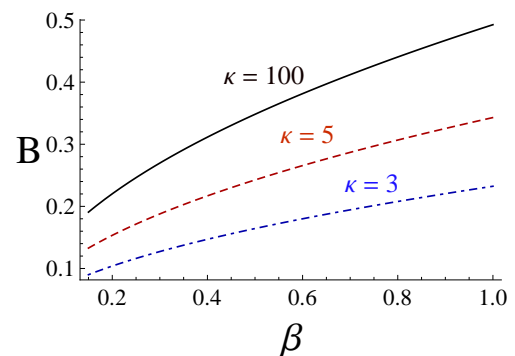
(b)

FIG. 3: (Color online) The nonlinearity coefficient A and the dispersion coefficient B are shown versus β for different values of κ. Here, the curves correspond, top to bottom, to: $\kappa = 100$ (solid black curve); $\kappa = 5$ (dashed red curve) and $\kappa = 3$ (dot-dashed blue curve).

V. KORTEWEG-DE VRIES EQUATION (CONSERVATIVE CASE)

It may be instructive, at this stage, to consider the conservative case ($\eta = 0$). In the absence of dissipation, the variable stretching adopted in the previous Section is generally associated to the Korteweg-de Vries (KdV) theory for small-amplitude potential pulses. We needn't iterate the algebraic details of the expansion procedure here, as these may be inferred, step by step, upon setting $C = 0$, i.e., by neglecting kinematic viscosity η at every step. As expected, the evolution equation thus obtained take the form of the KdV equation:

$$\frac{\partial \phi_1}{\partial \tau} + A\phi_1 \frac{\partial \phi_1}{\partial \xi} + B\frac{\partial^3 \phi_1}{\partial \xi^3} = 0\,, \qquad (25)$$

where the nonlinearity coefficient A and the dispersive coefficient B are given by expressions (22) and (23) above (these are depicted in Figs. 2 and 3).
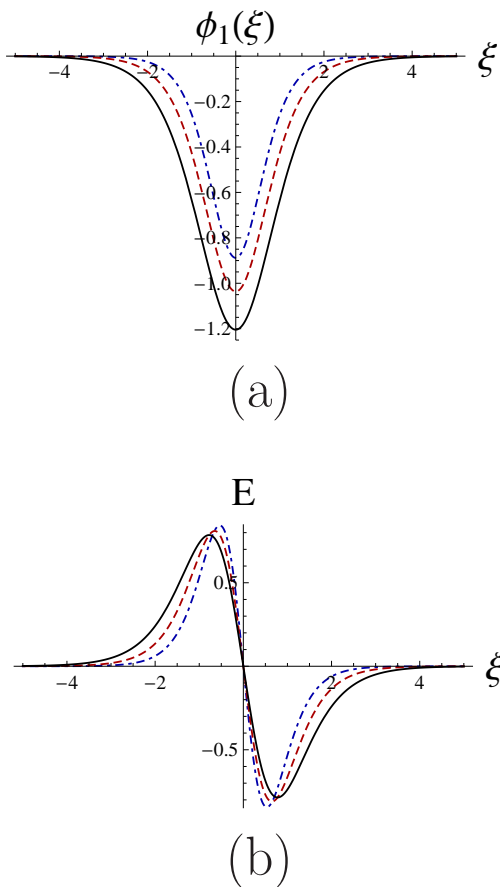
Solitary structures are sustained when dispersion

(a)

(b)

FIG. 4: (Color online) The electrostatic potential $\phi_1(\xi)$ (left panel) and the corresponding electric field E (right panel) are shown, as they result from Eq. (26) and (28), respectively. Three cases are depicted: strong superthermality, for $\kappa = 3$ (dot-dashed blue curve); $\kappa = 5$ (dashed red curve); quasi-Maxwellian case $\kappa = 100$ (solid black curve). The cold-to-hot electron ratio was taken to be $\beta = 0.5$ in both cases.

balances nonlinearity. The known one-soliton solution of the KdV equation bears the form:

$$\phi_1(\xi, \tau) = \phi_0 \, \text{sech}^2\left(\frac{\xi - V\tau}{L_0}\right) , \qquad (26)$$

where the pulse amplitude ϕ_0 and the pulse width L_0, defined as

$$\phi_0 = 3V/A , \qquad L_0 = \sqrt{4B/V} , \qquad (27)$$

satisfy the relation $\phi_0 L_0^2 = 12B/A$. Since A is negative, only negative potential pulses will occur; see Fig. 4a. The electric field $E = -\nabla\phi$ thus derived from the electrostatic potential $\phi_1(\xi, \tau)$ reads

$$E = \frac{6V}{AL_0} \, \text{sech}^2\left(\frac{\xi - V\tau}{L_0}\right) \tanh\left(\frac{\xi - V\tau}{L_0}\right) , \quad (28)$$

which represents a bipolar electric field excitation, as shown in Fig. 4b.

Expressions (26) and (27), in combination with the definitions (22) and (23) above, provide a diagnostic tool for superthermal plasmas: for a given value of the (assumed a priori measurable) potential pulse amplitude or/and width, the value of κ can be inferred from the above relations. Nonetheless, we see that only low (e.g., below $\kappa \simeq 6$) values of κ bear a noticeable effect.

We saw above (cf. Fig. 3) that superthermality results in higher values of $|A|$ (nonlinear coefficient, in absolute value) and smaller values of B. Therefore, solitary waves (potential pulses) in superthermal plasmas are expected to be of smaller amplitude and narrower width than in Maxwellian plasmas (refer to the definitions of ϕ_0 and L_0 above).

VI. ELECTRIC POTENTIAL SHOCK EXCITATION

The pulse solitons obtained in the previous Section were characterized by a vanishing electric potential at infinity. Let us now look for stationary profile solutions of the KdVB equation (21) in the form of *shock excitations*, possessing a fixed but finite (non-zero) limit at both infinities. Such a solution can be obtained via the hyperbolic tangent method [46–49], and the characteristics of the solution are discussed in detail in Ref. [50]. We therefore choose to omit unnecessary details here, yet providing the essential information in the following.

The exact solution of the KdVB equation (21) reads:

$$\phi_1(\xi, \tau) = \frac{V}{A} + \frac{3C^2}{25AB} \, \text{sech}^2\left(\frac{\xi - V\tau}{L}\right) - \frac{6C^2}{25AB} \tanh\left(\frac{\xi - V\tau}{L}\right). \qquad (29)$$

The parameter L entering the argument of the hyperbolic functions represents the width of the shock structure, which reads:

$$L = \frac{10B}{C} . \qquad (30)$$

The shock wave propagation speed V is related to the boundary conditions, as can be easily seen by considering the asymptotic values $\phi_1(\xi \to +\infty) = V/A -$

―――――

[2] One may choose to assign a zero value to one of the asymptotic values, e.g. at $+\infty$, as in Refs. [47, 48]. However, this then prescribes the value of V, and shifts all solutions (29) by a constant. It may also be pointed out that $\phi = 0$ at infinity (i.e., in regions far ahead of the propagating shock) is understood in the derivation of (25), and is thus a plausible requirement to impose (refer to the discussion in Ref. 50). For the sake of (algebraic) generality though (yet implying no loss in physical rigor), we chose to proceed by retaining arbitrary asymptotic values here.

$6C^2/25AB$ and $\phi_1(\xi \to -\infty) = V/A + 6C^2/25AB$. Combining the latter expressions, one obtains the shock wave amplitude Φ_0 in the form

$$|\Phi_0| = \frac{12C^2}{25|A|B} \ . \tag{31}$$

We stress that the above solution relies on dissipation to exist, and in fact collapses to a constant in the limit $C = 0$. There is no way to recover the pulse-shaped soliton (26) from (29), in any limit (this is not surprising, as different boundary values were assumed).

The qualitative effect of dissipation on the shock profile is evident. Note that the damping term C affects both Φ_0 and L, by resulting in steeper (narrower) and taller shocks, the higher its value. On the other hand, we remark that the product $|\Phi_0|L^2 = 48B/|A|$ is independent of C (which is reminiscent of a similar relation in KdV solitons).

Interestingly, since the sign(s) of B and C (both positive) and A (negative) is (are) prescribed in our case, only one polarity is possible, leading to the kink-shaped excitation depicted in the figures. In the general case, the sign of A would prescribe the polarity of the shock profile (bearing a kink- or an antikink-shaped form).

We note for rigor that, since the electric potential is determined up to a(n) (arbitrary, real) constant, being associated to an electric field $\mathbf{E} = -\nabla\phi$, the constant term in (29) can be omitted, without loss of physical meaning (yet against mathematical generality). On the other hand, either of the above (constant) asymptotic limits at $\xi \to \pm\infty$ can be set to zero[47], which simplifies the final expression (yet prescribing V in terms of A, B, C). An interested reader is referred to the rigorous discussion in Ref. 50. For the sake of generality, however, we have chosen to retain the general expression (29) above, which will be reflected in the diagrams discussed in the Section VII.

The relative magnitude (and the sign) of the coefficients in the KdVB equation will determine the interplay among dispersion, nonlinearity and dissipation, lying in the heart of our physical problem. Their parametric dependence on relevant physical parameters is depicted in Figs. 2 and 3. As discussed above, the dispersion coefficient acquires smaller values while, inversely, the (absolute value of the) nonlinearity coefficient acquires higher values for stronger superthermality; dissipation may thus easily become dominant after a change in κ (e.g., due a local disturbance in the plasma properties), resulting in narrower/steeper [cf. (30)] and taller [cf. (31)] shocks the stronger the damping - a typical feature in the dynamics of shock waves. A similar trend is witnessed for lower values of the cold-to-hot electron density ratio β, suggesting that the more the hot (superthermal) electrons, the lower dispersion (and the stronger nonlinearity) will be, and thus the steeper and taller the shock profile will be. On the other hand, the damping term C is

constant, i.e., it depends only on the electron kinematic viscosity η (and not on κ, nor on the plasma composition via β).

It is straightforward to obtain an expression for the electric field $\mathbf{E} = -\nabla\phi$ from the above expression (29):

$$E = \frac{6C^2}{25ABL} \operatorname{sech}^2\left(\frac{\xi - V\tau}{L}\right)\left[1 + \tanh\left(\frac{\xi - V\tau}{L}\right)\right]. \tag{32}$$

This form represents an inverse-bell-shaped (since $A < 0 < B$) monopolar localized excitation for the electric field. Obviously, the above discussion on the width L also holds here, so steeper electric potential disturbances should lead to narrower electric field pulses, while the same holds for the maximum pulse amplitude $\sim C^2/|A|B$ as obtained from (32); cf. (31).

VII. PARAMETRIC INVESTIGATION

We may now investigate the dynamical properties of electron-acoustic excitations in terms of the intrinsic parameters of our model, namely the cold-to-hot electron density ratio β, the superthermality parameter κ and the (cold electron) kinematic viscosity η (i.e., dissipation via $C \sim \eta_0$). We adopt values of the cold-to-hot electron density ratio β in the range $0.25 - 4$, where Landau damping is mimimized [4, 7, 9].

Phase velocity. The dependence of the EA phase velocity [defined in (10)] on excess electron superthermality (via κ) and on the electron density ratio β is explored in Fig. 1. The (weak) kinematic viscosity does not enter the dynamics at the linear level. The superthermality parameter κ and the cold-to-hot electron density ratio β play an important role on the linear behavior of EAWs. The EA phase speed increases as $\sim \sqrt{\beta}$ for fixed κ, since, having more inertial (cold) electrons (as compared to the superthermal electrons) allows for increased inertia to sustain the waves, which i.e., leads to a higher phase velocity. On the other hand, keeping β fixed, the EA phase speed decreases with higher superthermality, i.e., for lower κ; see Fig. 1b.

Effect of superthermality (via κ). The nature of the electrostatic EA shock profile is significantly affected by superthermality of the considered plasma, as clearly shown in Fig. 5 (where we have considered a fixed value of β and of $\eta_0 \sim C$). As expected, a taller and steeper shock profile results from higher superthermality (lower κ).

The dissipation term only depends on the electron kinematic viscosity, whereas the dispersion term depends on the cold-to-hot electron density ratio and on the superthermality parameter κ. For any fixed value of β, the dispersion term decreases with lower κ, i.e., dispersion becomes weaker for stronger superthermality. As a result, dissipation dominates on EA shock dynamics for stronger superthermality (as dispersion fails to balance) and allows for the formation of higher
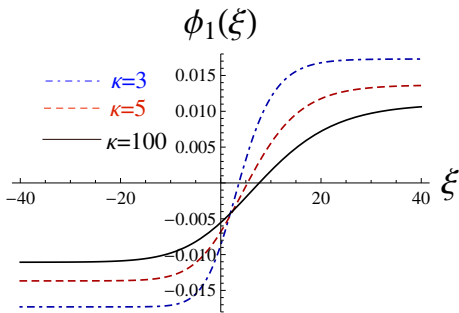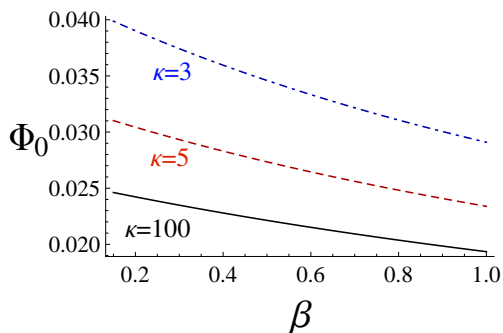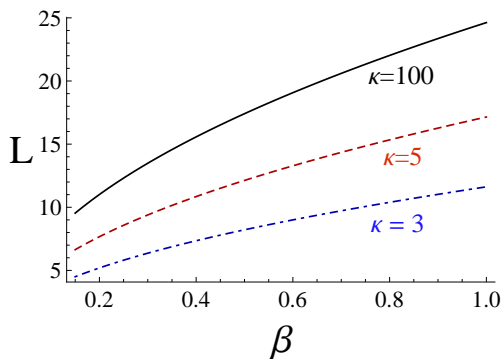
FIG. 5: (Color online) The electron-acoustic shock profile given by Eq. (29) is depicted versus the space coordinate ξ, for different values of the superthermality parameter κ. We have taken $\beta = 0.5$ and $\eta_0 = 0.4$.

(a)

(b)

FIG. 6: (Color online) The variation of the shock wave (a) amplitude Φ_0, as given in Eq. (31), and (b) width L, as given in Eq. (30) with β is depicted for different κ, here $\eta_0 = 0.4$ in both cases.

amplitude and steeper shock waves. The effect of superthermality on the shock amplitude (left panel) and width (right panel) is depicted in Fig. 6. We see that the stronger superthermality (lower κ) effect, the larger and narrower the shocks will be.

Cold-to-hot electron density ratio (β) effect. The ef-

fect of the cold-to-hot electron density ratio β on the shock profile is explored in Fig. 7 (keeping the values of κ and η_0 fixed), which shows the spatial variation of the electrostatic shock for different values of β. We see that β has a strong influence on the shock wave amplitude and width. As discussed above, one witnesses a larger (in amplitude) and narrower (in width) shock profile for lower β. Therefore, considering a higher population of cold electrons results in smaller but wider shock structures.
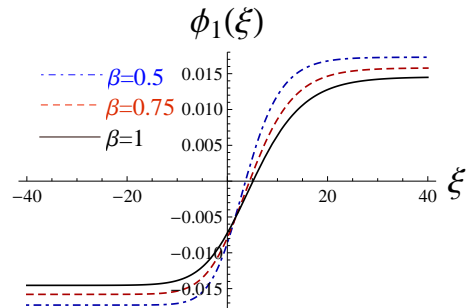
FIG. 7: (Color online) The shock profile is depicted (versus the space coordinate ξ) for different values of the cold-to-hot electron density ratio β, taking $\kappa = 3$ and the electron kinematic viscosity $\eta_0 = 0.4$.

The geometric characteristics of the shock excitations are investigated in Fig. 8. The amplitude Φ_0 is smaller, while the width L is larger, for higher values of β, i.e., for a more significant cold-electron population; see Fig. 8a, b, respectively.

Effect of kinematic viscosity (via η_0). Fig. 9 illustrates the effect of kinematic viscosity on the EA shock profile. Stronger (larger amplitude, steeper) shocks are predicted for higher η_0.

Finally, the shock wave amplitude and width are depicted in Fig. 10 versus β, for different values of the cold electron kinematic viscosity η_0 (keeping all other relevant parameters fixed; in particular, $\kappa = 3$ was taken in this plot). We see that, as discussed above, higher values of the kinematic viscosity result in larger-amplitude (see Fig. 10a) and narrower (see Fig. 10b) shock waves.

VIII. NUMERICAL SIMULATION

We have analyzed the propagation of EA solitary structures and shocks by a numerical integration of the KdV and the KdVB Equation(s), respectively, employing a Runge-Kutta 4 method. We have retained as an intrinsic element in our code the dependence of the coefficients on the superthermality parameter κ and on β, as in our analytical model. A time interval 10^{-4} and a spatial grid size 0.1 were considered.

As a possible scenario in the dynamics, we have chosen to investigate the response of a stable pulse
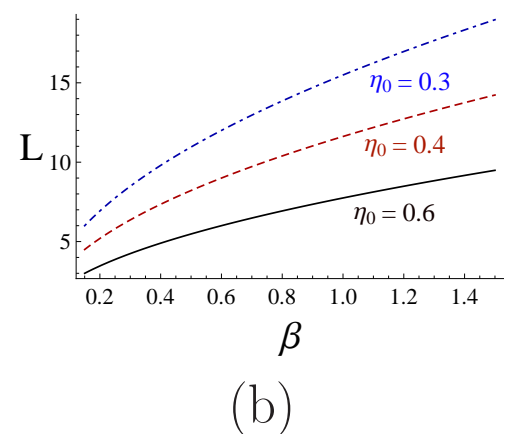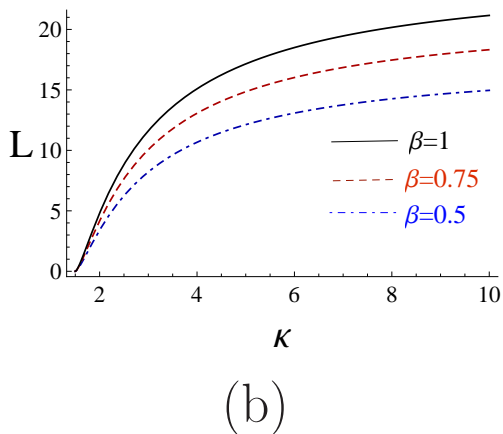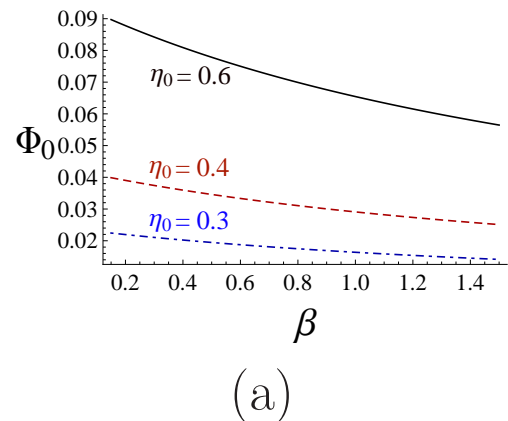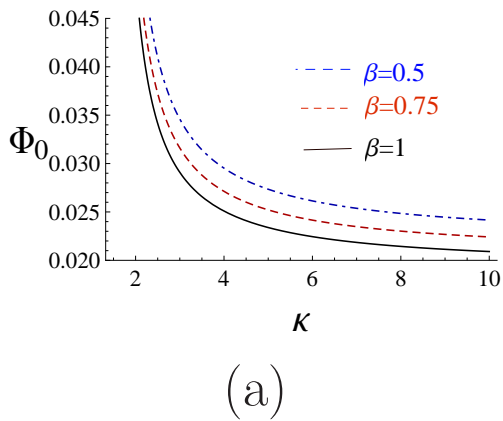
FIG. 8: (Color online) The dependence of the shock wave (a) amplitude Φ_0 (in Eq. (31)) and (b) width L (in Eq. (30)) with the superthermality parameter κ is shown, for different β; here $\eta_0 = 0.4$.
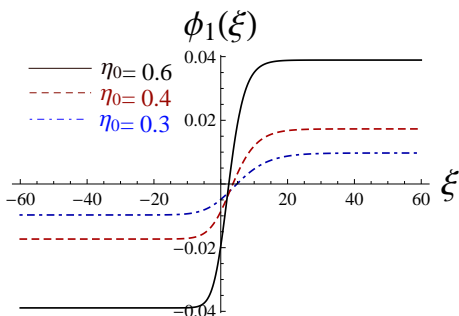

FIG. 9: (Color online) The shock profile is depicted (versus the space coordinate ξ) for different kinematic viscosity η_0, taking $\kappa = 3$ and $\beta = 0.5$.


FIG. 10: (Color online) The dependence of the shock wave (a) amplitude Φ_0 (in Eq. (31)) and (b) width L (in Eq. (30)) on the cold-to-hot electron density ratio β is depicted, for different cold electron kinematic viscosity η_0; here we have taken $\kappa = 3$.

propagating in (i.e., an exact solution sustained in) Maxwellian plasma, when it encounters a region with a strong deviation of the hot electrons from thermal equilibrium (lower κ value). To this end, we have considered the pulse soliton solution (26) for $\kappa = 100$ as initial condition. This (same) potential pulse was used as initial condition in three simulations. First, integrating the KdV equation for a high (quasi-Maxwellian) value of κ ($= 100$), we have confirmed the stability of the pulse (expected, as this was an exact solution for $\kappa = 100$); see Figs. 11a and 12a. Subsequently, we have considered two lower values, namely $\kappa = 5$ and $\kappa = 3$. The profiles obtained numerically are shown in Figure 11. We note here that this is an idealized assumption. Spatial changes in the electron distribution tend to equilibrate rapidly and we can not expect a sharp boundary between two regions with very different electron velocity distributions.

In the former case ($\kappa = 5$), depicted in Figs. 11b and 12b, the initial pulse is seen to decompose into a different (thinner, steeper) pulse, which remains stable (beyond some initial transition period), followed by a sea of harmonic oscillations. The interpretation of this observation is straightforward: we have argued above that a small change in kappa destabilizes the soliton, as it bears opposite effects on dispersion and nonlinearity coefficients, which thus fail to balance.
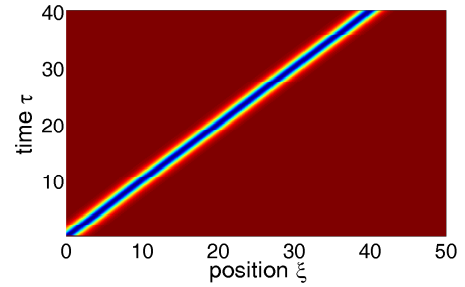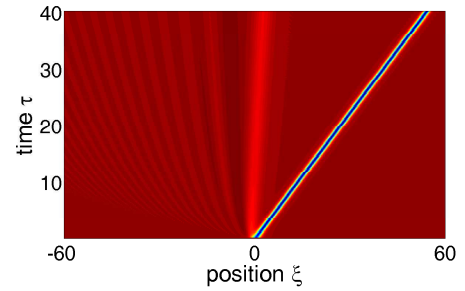
(a)

(a)

(b)

(b)

(c)
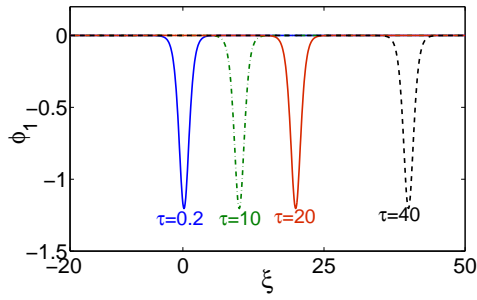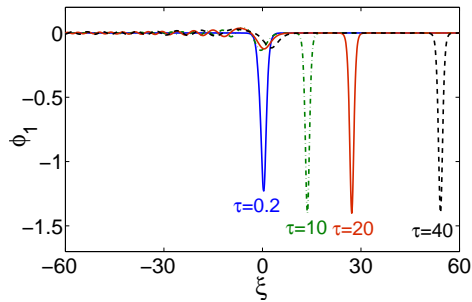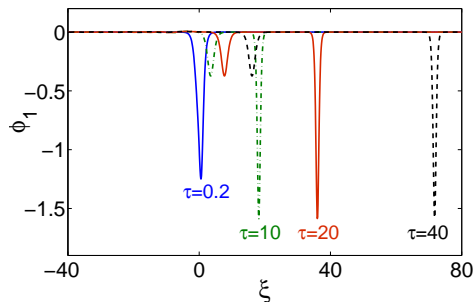
(c)

FIG. 11: (Color online) Evolution of electrostatic solitary structures (given in Eq. (25)) propagating in: (a) Maxwellian plasma ($\kappa = 100$); (b) a mildly nonthermal plasma ($\kappa = 5$); (c) a strongly nonthermal plasma ($\kappa = 3$). The exact solution (26) was considered as initial condition, for $\kappa = 100$ (i.e. Maxwellian), in all three simulations. We have set $V = 1$ and $\beta = 0.5$ everywhere.

FIG. 12: (Color online) Propagation of a solitary wave (given in Eq. (25)) in the space-time plane for similar condition as Fig. 11.

The energy stored in the pulse may nevertheless be sufficient to form a smaller (energetically speaking) pulse, and the remaining amount of energy is carried by periodic oscillations.
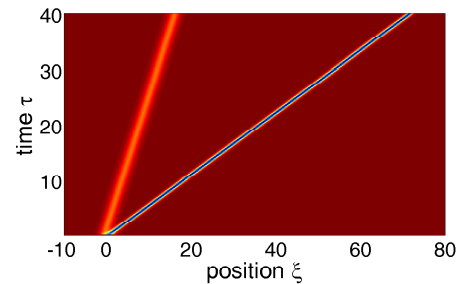
In the latter case ($\kappa = 3$), however (depicted in Figs. 11c and 12c), the initial pulse is seen to decompose exactly into a pair of pulses: a dominant (thin-

ner, steeper) fast pulse, followed by a smaller (and slower) one. Again, this is due to a delicate energetic balance having been achieved, as the initial condition succeeds in providing the energy necessary for the formation of a two-soliton configuration, which appears to propagate in a stable manner (and presumably coincides with a two-soliton solution of the integrable KdV equation).

The inverse transition is considered in Fig. 13, where a pulse (an exact soliton solution) obtained for a superthermal environment ($\kappa = 3$) is assumed to enter a "Maxwellian" ($\kappa = 100$) region. In our simulation,
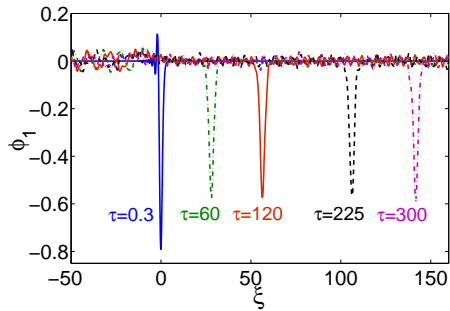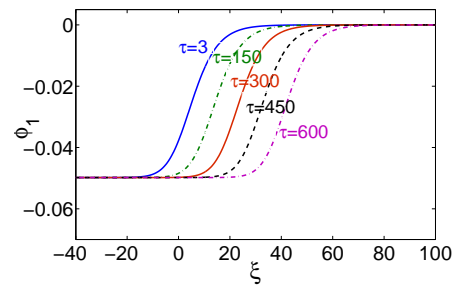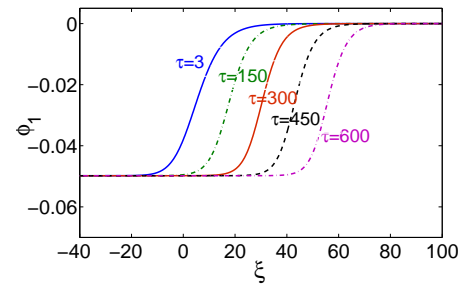
(a)
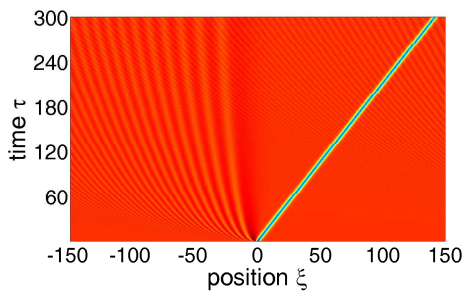
(b)

FIG. 13: (Color online) (a) Evolution of the electrostatic solitary structures (given in Eq. (25)) propagating in a Maxwellian plasma ($\kappa = 100$). Here, Eq. (26) was considered as initial condition, for $\kappa = 3$ (i.e. superthermal), where $V = 1$ and $\beta = 0.5$; and (b) showing the propagation in the space-time plane for same condition as panel (a).

(a)

(b)

FIG. 14: (Color online) Evolution of the electrostatic shock solution given by Eq. (21) (for $\kappa = 100$) propagating in (a) a "Maxwellian" plasma ($\kappa = 100$), and (b) a superthermal plasma ($\kappa = 3$). Eq. (29) is considered as initial condition for $\kappa = 100$ and $\beta = 0.5$, $C = 0.3$ in both cases.

shown in Fig. 13, we have considered the exact soliton solution given in Eq. (26) for $\kappa = 3$ as initial condition, while the KdV equation integrated numerically was considered for $\kappa = 100$. In this case (see Fig. 13), the soliton adapts its shape by initially losing energy to the medium (via random fluctuations which later smear out), and then eventually stabilizing to a new (shorter, wider) pulse configuration, which appears to be sustained for as long as the simulation ran.

We have carried out a similar investigation for electrostatic shock fronts, relying on the exact solution of Eq. (21), given by Eq. (29), as initial condition for $\kappa = 100$ (we have considered $V = 6C^2/25B$ here, in account of a vanishing potential at positive infinity). The result is shown in Fig. 14. The shock is seen to maintain its stability (constant amplitude and width) while propagating in a Maxwellian plasma, i.e. when Eq. (21) is also considered for $\kappa = 100$: see Fig. 14a. When the same shock profile (also adopted as initial condition in Fig. 14b) enters a superthermal ($\kappa = 3$) plasma region, it is seen to adapt its width to the new environment, and in fact slightly accelerates, but oth-

erwise suffers no other major structural change. The acceleration of shocks when entering a lower-κ region can be physically attributed to the excess superthermal hot electrons surrounding them. This is anticipated, due to the modification of the sound speed of EA waves (cf. Fig. 1a), which results in an energy surplus available for lower κ within the superacoustic shocks.

In order to investigate the role of the damping coefficient, we have considered a solution of the KdVB Eq. (21) in the form of (29), as obtained for $C = 0.1$, suffering a sudden increase in the value of C. To simulate this situation, we adopt the latter solution as initial condition to integrate the KdVB Eq. (21) numerically, yet for a higher value of C ($= 1$). We see that the shock adapts its shape to the new situation by stretching its spatial extension, yet otherwise suffers no other change in characteristics, as depicted in Fig. 15.

The situation considered here is admittedly rather idealized. Spatial changes in the electron distribution tend to equilibrate rapidly and we can not expect a sharp boundary between two regions with very
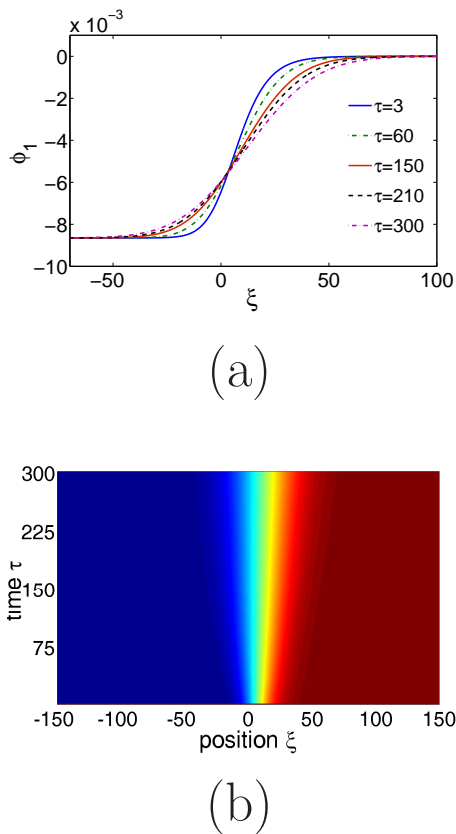
(a)

(b)

FIG. 15: (Color online) Evolution of the shock solution of Eq. (21) as given by (29), propagating in a superthermal plasma ($\kappa = 3$), which is highly dissipative (taking $C = 1$). Eq. (29) is considered as initial condition for $\kappa = 3$, $C = 0.1$. We have taken $\beta = 0.5$ everywhere.

different electron velocity distributions. Nonetheless, our aim was to test the robustness and stability of electron-acoustic shocks against a change in the electron velocity distribution. In this sense, our conclusion that shocks are remarkably stable against changes in the thermal distribution is important.

IX. CONCLUSIONS

The nonlinear propagation of electron-acoustic shock wave was investigated in a plasma characterized by a superthermal (non-Maxwellian) electron population. A three-component-plasma fluid model was employed, comprising inertial ("cold") electrons, inertialess superthermal ("hot") electrons, and stationary ions. A κ (kappa) type distribution function was employed to model the nonthermal (hot) electron component. The kinematic viscosity of the (cold) electron population was taken into account.

A Korteweg-de Vries–Burgers (KdVB) type nonlinear evolution equation was derived for the electrostatic potential via a reductive perturbation method, and then analyzed analytically and numerically. A Korteweg-de Vries (KdV) equation was obtained in the conservative (dissipationless) case. Exact solutions of the KdVB equation were obtained, bearing a monotonic kink-shaped shock profile sustained by dissipation. A negative pulse solution was obtained through the KdV description. The nonlinearity and dispersion coefficients were shown to depend on plasma configurational parameters (κ, β), while the damping coefficient was assumed to be constant. The parametric dependence of the shock profile on the plasma concentration (cold-to-hot electron density ratio) and in particular, on the level of excess electron superthermality was investigated. The nonlinearity coefficient was found to acquire higher values, while the dispersion coefficient takes smaller values for stronger superthermality (lower κ), a fact that suggests that the shocks formed will be narrower/steeper and stronger, compared to the Maxwellian case. A similar trend was witnessed for lower values of the cold-to-hot electron density ratio (β), suggesting that the more the hot (superthermal) electrons are dominant, the steeper and taller the shock profile will appear. In highly nonthermal situations, wave damping dominates over dispersion and nonlinearity, thus resulting in the formation of narrower and stronger shock excitations.

Our theoretical predictions were tested numerically. A hypothetical situation in which a stable pulse (exact solution) propagating in a Maxwellian plasma enters a "nonthermal region" (characterized by smaller κ) was considered. The energy stored in the pulse was the distributed into a smaller pulse, followed by waves, or (if the energy balance permits)) into a stable multi-soliton configuration. Of course, is due to the KdV equation providing a conservative system, known to possess an infinite hierarchy of (multi-)soliton solutions at different energy levels. The inverse scenario (a stable pulse for small κ entering a high κ region) was shown to lead to decay of the pulse through random oscillations (noise).

The stability of the shock profile has been tested numerically and it has been observed that the shock was seen to affect its shape, but not its stability profile while passage from high to low values of κ.

Our results may be useful in understanding the behavior of Space or laboratory plasmas which are characterized by a secondary population of energetic (superthermal) electrons.

Natal, Durban, South Africa), Prof Frank Verheest (Gent Universiteit, Belgium) and Dr Nareshpal Saini (Guru Nanak Dev University, India).

---

[1] K. Watanabe and T. Taniuti, J. Phys. Soc. Jpn. **43**, 1819 (1977).
[2] M. Y. Yu and P. K. Shukla, J. Plasma Phys. **29**, 409 (1983).
[3] R. L. Tokar and S. P. Gary, Geophys. Res. Lett. **11**, 1180 (1984).
[4] R. L. Mace and M. A. Hellberg, J. Plasma Phys. **43**, 239 (1990).
[5] I. Kourakis and P. K. Shukla, Phys. Rev. E **69**, 036411 (2004).
[6] A. A. Mamun, P. K. Shukla and L. Stenflo, Phys. Plasmas **9**, 1474 (2004).
[7] S. P. Gary and R. L. Tokar, Phys. Fluids **28**, 2439 (1985).
[8] R. L. Mace, G. Amery and M. A. Hellberg, Phys. Plasmas **6**, 44 (1999).
[9] T. K. Baluku, M. A. Hellberg and R. L. Mace J. Geophys.Res. **116**, A04227 (2010), doi:10.1029/2010JA016112.
[10] H. Rothkaehl *et al*, Adv. Space Res. **43**, 948 (2009).
[11] D. S. Montgomery *et al*, Phys. Rev. Lett. **87**, 155001 (2001).
[12] Quanming Lu, Shui Wang, and Xiankang Dou, Phys. Plasmas. **12**, 072903 (2005).
[13] M. E. Dieckmann, A. Bret and P. K. Shukla, Plasma Phys. Contr. Fusion **49**, 1989 (2007).
[14] A. A. Mamun and P. K. Shukla, J. Geophys. Res. **107**, SIA 15-1 (2002).
[15] P. K. Shukla, A. A. Mamun and B. Eliasson, Geophys. Res. Lett. **31**, L07803 (2004).
[16] E. K. El-Shewy, Chaos, Solitons and Factrals **34**, 628 (2007).
[17] S. Younsi and M. Tribeche, astrophys. Space Sci. **330**, 295 (2010).
[18] A. Danehkar, N.S. Saini, M.A. Hellberg, and I. Kourakis, Phys. Plasmas **18**, 072902 (2011).
[19] S. V. Singh and G. S. Lakhina, Nonlin. Process Geophys. **11**, 275 (2004).
[20] H. Matsumoto, H. Kojima, T. Miyatake, *et al.*, Geophys. Res. Lett. **21**, 2915 (1994).
[21] R. E. Ergun, C. W. Carlson, J. P. McFadden *et al.*, Geophys. Res. Lett. **25**, 2041 (1998).
[22] J. S. Pickett, D. A. Gurnett, J. D. Meyietti *et al.*, Adv. Space Res. **24** (1), 23 (1999).
[23] N. Dubouloz, R. Pottelette, M. Malingre, G. Holmgren, P. A. Lindqvist, *J. Geophys. Res.* **96**, 3565 (1991).
[24] S. Sultana and I. Kourakis, Plasma Phys. Control. Fusion **53**, 045003 (2011).
[25] C. Vocks and G. Mann Astrophys. J. **593**, 1134 (2003).
[26] G. Gloeckler and L. A. Fisk, Astrophys. J. **648**, L63 (2006).
[27] C. Vocks, G. Mann and G. Rausche, Astronomy & Astrophysics **480**, 527 (2008).
[28] S. Preische, P. C. Efthimion and S. M. Kaye, Phys. Plasmas **3**, 4065 (1996).
[29] Y. Yagi *et al*, Plasma Phys. Cont. Fusion **39**, 1915 (1997).
[30] S. Magni *et al*, Phys. Rev. E **72**, 026403 (2005).
[31] V. M. Vasyliunas, J. Geophys. Res. **73**, 2839 (1968).
[32] D. Summers and R. M. Thorne, Phys. Fluids. **B 3**(8), 1835 (1991).
[33] M. A. Hellberg *et al*, Phys. Plasmas **16**, 094701/1-5 (2009).
[34] S. Sultana, I. Kourakis, N. S. Saini and M. A. Hellberg, Phys. Plasmas **17**, 032310 (2010).
[35] R. L. Mace and M. A. Hellberg, Phys. Plasmas **2**, 2098 (1995).
[36] M. A. Hellberg, R. L. Mace, R. J. Armstrong and G. Karlstad, J. Plasmas Phys. **64**, 433 (2000).
[37] K. Roy, A. P. Misra and P. Chatterjee, Phys. Plasmas **15**, 032310 (2008).
[38] J. K. Xue, Phys. Lett. A **322**, 225 (2004).
[39] P. K. Shukla and A. A. Mamun, IEEE Trans. Plasma Sci. **29**, 221 (2001).
[40] A. A. Mamun and P. K. Shukla, Physics Sripta T **98**, 107 (2002).
[41] B. Sen, B. Das and P. Chatterjee, Eur. Phys. J. D **49**, 211 (2008).
[42] J. K. Xue, Phys. Plasmas **10**, 4893 (2003).
[43] A. L. Velikovich *et al*, Phys. Plasmas **8**, 4524 (2001); refer to Eq. (5) and Fig. 1 therein
[44] H. Washimi and T. Taniuti, Phys. Rev. Lett. **17**, 996 (1966).
[45] P. K. Shukla and A. A. Mamun, New J. Phys. **5**, 17.1 - 17.37 (2003).
[46] A. Jeffrey and S. Xu, wave motion **11**, 559 (1989).
[47] W. Malfliet and W. Hereman, Physica Scripta **54**, 563 (1996).
[48] A. M. Wazwaz, Appl. Math. Comput. **154**, 713 (2004).
[49] H. Demiray, Wave Motion **38**, 367 (2003).
[50] I. Kourakis, S. Sultana and F. Verheest, Astrophys. Space Sci. DOI 10.1007/s10509-011-0958-5.